



ELSEVIER

Thermochimica Acta 322 (1998) 95–100

thermochimica
acta

Structural stability of actin filaments as studied by DSC and EPR

D. Lőrinczy^{a,*}, F. Könczöl^b, B. Gaszner^c, J. Belagyi^c^a Biophysical Institute, University Medical School of Pécs, Szigeti u. 12, H-7643 Pécs, Hungary^b Institute of Forensic Medicine, University Medical School of Pécs, Szigeti u. 12, H-7643 Pécs, Hungary^c Central Research Laboratory, University Medical School of Pécs, Szigeti u. 12, H-7643 Pécs, Hungary

Received 17 June 1998; received in revised form 16 July 1998; accepted 21 July 1998

Abstract

Thermal stability of actin, isolated from skeletal muscle, was studied in monomeric and polymerized form using DSC and EPR spectroscopy. The analysis of the DSC profiles in both forms enabled the assignment of the components: two endothermic components in the G-form ($47.3 \pm 1.4^\circ\text{C}$ and $53.4 \pm 1.8^\circ\text{C}$ with enthalpies of 184.4 ± 10.9 and 120.0 ± 7.5 kJ/mol), and three endothermic components in the F-form ($T_{m1} = 59.7 \pm 1.4^\circ\text{C}$, $H_1 = 171.3 \pm 1.7$ kJ/mol; $T_{m2} = 60.6 \pm 1.6^\circ\text{C}$, $H_2 = 231.2 \pm 9.6$ kJ/mol; $T_{m3} = 61.3 \pm 1.4^\circ\text{C}$, $H_3 = 148.3 \pm 4.6$ kJ/mol).

Actin was labeled with the paramagnetic derivative of maleimide at the reactive thiol site Cys-374 in the C-terminal subdomain-1. The rotational correlation time for MSL-F-actin is 100 μs , as obtained from the peak ratio $L''/L = 0.745 \pm 0.05$ ($n=6$), which indicates that there is significant internal flexibility in F-actin. The unfolding of actin induced by heating resulted in a single transition in both forms of actin.

The comparison of G- and F-actins showed remarkable differences in transition temperature and enthalpy, suggesting intramolecular interactions between subdomains and monomers. © 1998 Elsevier Science B.V.

Keywords: DSC; EPR; G-actin; F-actin; Thermal unfolding

1. Introduction

Actin is one of the major components in the micro-filament system of the eucaryotic cells. It is involved in many cellular processes, such as the maintenance of cell shape, cytoplasmic streaming, axonal transport and cell division [1,2]. The ability of actin monomers (G-actin) to polymerize into filamentous form (F-actin) is crucial in structural and motile functions of the cells. A major role of actin lies in the generation of force by striated and smooth muscle cells. The

mechanism of muscle contraction which is fuelled by the hydrolysis of ATP has been investigated from many points of view, and presently it is understood in considerable detail.

In general, the protein function largely depends on the internal flexibility and the time scale of the internal motion. These properties are influenced by such environmental factors as temperature, ionic strength, pH and concentration of proteins. The conformation of monomeric actin changes when it is incorporated into filaments, and an internal structural rearrangement can be assumed when myosin binds to actin [3–5]. Some properties of actin filaments are possibly important in the dynamics of actin-containing structures as well.

*Corresponding author. Tel./Fax: +36-72-314017; e-mail: microcal@apacs.pote.hu

The in-vitro dynamic properties of actin filaments can be studied by different experimental techniques. The conformational changes associated with alteration of the structural stability of the protein can be studied by DSC and electron paramagnetic resonance (EPR) spectroscopy under different conditions. The simultaneous application of DSC and EPR has the advantage that both, local and global conformational changes can be detected [6,7].

The aim of the present work was to investigate the thermal stability of the two G- and F-forms of actin and to find the relationship between internal flexibility and thermodynamic data.

2. Materials and methods

2.1. Preparation of actin

The preparation procedure of actin from skeletal muscle for DSC and EPR measurements was described in an earlier paper [7]. Briefly, actin was extracted from an acetone-dried powder of rabbit back and leg muscles according to the method of Spudich and Watt [8]. The composition of the extraction solution was 0.2 mM ATP, 0.2 mM CaCl₂, 1.5 mM NaN₃ and 2 mM HEPES (pH 8.3). The crude actin was purified by two polymerization–depolymerization cycles to remove contaminated proteins.

2.2. Spin labelling of actin

Spin labelling of actin was performed in filamentous form in a solution containing 100 mM KCl, 2 mM MgCl₂ in 2 mM HEPES buffer at pH 8.3 with 1.2 mol of 4-maleimido-2,2,6,6-tetramethylpiperidinoxyl (MSL) per mole of actin for 90–120 min at 0°C. The molecular weight of actin monomer was assumed to be 42 kD. Actin has a reactive cysteine residue (Cys-374) in subdomain-1 that can be labelled specifically with MSL. After spin labelling, the protein was centrifuged at 100 000×g for 1.5 h at 2°C to remove unreacted labels and to obtain pellet. The actin pellet was gently homogenized in 0.2 mM ATP 0.2 mM CaCl₂ and 2 mM HEPES (pH 8.3) and the homogenizate was dialyzed for 36 h against the extracting solution at 4°C. The conventional and saturation transfer EPR spectra were taken on samples in the

concentration range of 50–150 μM to obtain appropriate signal intensity in the saturation transfer EPR time domain. The concentration of the protein solution was determined by measuring the optical absorption with a Hitachi 124 spectrophotometer. The absorbance of monomer actin was taken as E^{280} (0.1%)=0.63.

2.3. EPR measurements

Conventional and ST EPR spectra were taken with an ESP 300E (Bruker, Germany) spectrometer. The first harmonic, in-phase, absorption spectra were obtained using 20 mW microwave power and 100 kHz field modulation with amplitude of 0.1–0.2 mT. The second harmonic, 90° out-of-phase, absorption spectra were recorded with 63 mW and 50 kHz field modulation of 0.5 mT amplitude detecting the signals at 100 kHz out-of-phase. The 63 mW microwave power corresponds to an average microwave field amplitude of 0.025 mT in the central region of the standard Zeiss tissue cell (Carl Zeiss, Germany), and the values were obtained using the standard protocol of Fajer and Marsh [9]. The spectra were recorded at a temperature of (22±1)°C, and the sample was thoroughly mixed on the surface of the flat cell before measurements in order to avoid the orientational effect in the sample that could arise from side-to-side filament–filament association into larger domains. The spectra were normalized to the same number of unpaired electrons calculating the double integral of the derived spectra.

In order to obtain a precise phase setting using saturation transfer (ST) EPR technique, a new procedure was applied. The idea of this procedure originates from B.H. Robinson (Department of Chemistry, Nashville University). Assuming that the variance of the EPR signal over the whole magnetic field scan at exact out-of-phase setting is zero at low microwave power (ca. 0.0025 mT), a phase angle (φ) can be calculated from two high-power EPR spectra with high accuracy. Two spectra (ε , $\varepsilon+90^\circ$, where ε is an arbitrary phase angle) are recorded on the same sample, and the difference between the phase angles must be exactly 90°. Simple linear transformation of the digitized spectra by the calculated phase angle (φ) allows the estimation of the second harmonic in-phase and out-of-phase EPR spectra. This method is called the *variance method*.

The procedure was tested on MSL-haemoglobin with different rotational correlation times in the ST EPR time domain and on glycerinated muscle fibres, labelled with maleimide or isothiocyanate spin labels.

2.4. DSC measurements

The thermal unfolding of actin in different states induced by KCl and $MgCl_2$ was monitored by a Setaram Micro DSC-II calorimeter. All experiments were performed between 5° and 80°C. The heating rate was 0.3°C/min. Conventional Hastelloy batch vessels were used during the denaturation experiments with 850 μ l sample volume, on average. The buffer solution for polymerized actin was used as reference sample. The sample and reference vessels were equilibrated with a precision of ± 1 mg. There was no need to do any correction from the point of view of heat capacity between the sample and reference vessels.

3. Results and discussion

3.1. Calculation of the phase angle

Fig. 1 shows the comparison between the adjusted and calculated phase angles. The results were obtained on MSL-haemoglobin samples that were subsequently measured with the variance method. The straight line was calculated by the least-squares method. The good fit (regression coefficient: $b=0.980\pm 0.035$, $n=14$, correlation coefficient: $R=0.992$) gives evidence that the variance method results in the same phase angle as the null method, within the limits of experimental error. The method seems to be useful, especially when larger proteins with low concentration of spin labels require detection. At a low concentration of free radicals where the null method yields rather poor signal-to-noise sensitivity, a high receiver gain is required, and in this case it is not easy to achieve the proper zero signal output at low microwave power.

In a series of measurements ($n=9$) on different muscle fibres (the wet mass of the fibres was ca. 30 mg and the degree of labelling varied between 0.3–0.4 mol label/mol myosin), the phase setting adjusted by the null method ($\varphi=0^\circ$) was changed by 40° and the spectra were taken; thereafter, the

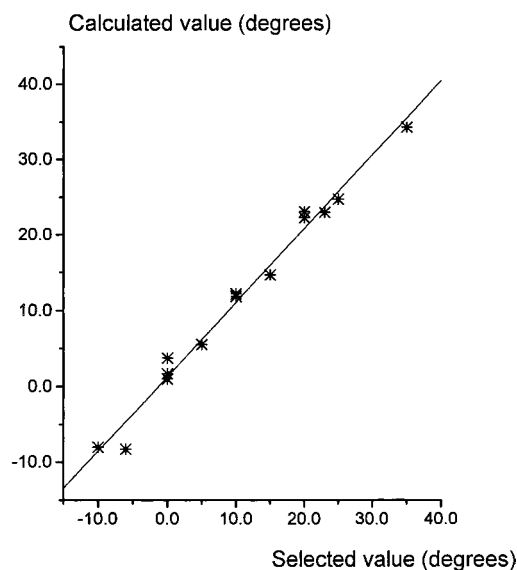


Fig. 1. Validity of the variance method. In a set of experiments on MSL-hemoglobin, the phase angle (φ) was determined by the null method, and then two high-power ST EPR spectra were recorded at $\varphi-\varepsilon$ and $\varphi-\varepsilon+90^\circ$ phase angles, where $\varepsilon<90^\circ$ is an arbitrary selected angle. The calculated phase angles are plotted as a function of the selected ε angle. The regression coefficient is close to the one evidencing the validity of variance method.

phase angles were calculated by the variance technique on each sample. The result of the measurements was $\varphi=42.38\pm 2.09$ (mean \pm standard deviation).

The comparison of the results with the previous methods (null and integral methods) shows that the variance method is nearly equivalent to the others and has an outstanding stability [10–12].

3.2. Stability of actin

Previous X-ray crystallographic studies of actin established that it is a multisubunit protein consisting of distinct domains that can produce coupled movements induced by the binding of myosin, nucleotide and divalent cations [13,14]. It is suggested from this mechanism that the thermally averaged conformation of actin is perturbed in the contractile process and other cell functions. The architecture of the molecule requires changes of the internal flexibility, and conformational changes are expected when the actin monomers are polymerized into filamentous actin. Further, structural changes can occur when myosin

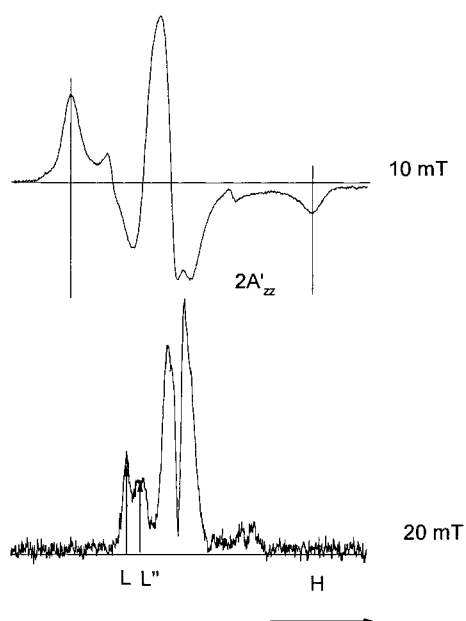


Fig. 2. Conventional and saturation transfer EPR spectra of F-actin. Actin was labelled with MSL in the F-form, the molar ratio of MSL to F-actin was 0.38. The parameters which were used for evaluation of the spectra are shown. The concentration of F-actin was 120 μ M.

binds to actin during the ATP hydrolysis cycle accompanying the generation of force [15].

The conventional and saturation transfer EPR spectra of F-actin is shown in Fig. 2. The spectra were taken after an hour of polymerization. As shown in Fig. 3, the polymerization of globular actin into filamentous actin is a fast process, but the process is not exactly complete after one hour. Former experiments on actin have shown that the polymerization is complete after 24 h as tested on spin-labelled gizzard actin [4]. The rotational correlation time for MSL-F-actin is 100 μ s obtained from the ratio $L''/L=0.745\pm 0.05$ ($n=6$) which indicates that there is significant internal flexibility in F-actin. The rotational correlation time is much faster than the characteristic times for the twisting and bending motion of the whole filament, and the latter has a biphasic character induced by heavy meromyosin [15]. Internal dynamics of proteins that is the result of correlated motions involving the localized atomic fluctuations of the protein structure is important in biological function [16], especially those collective motions that are usually coupled with functionally distinct states of proteins. The time scale of

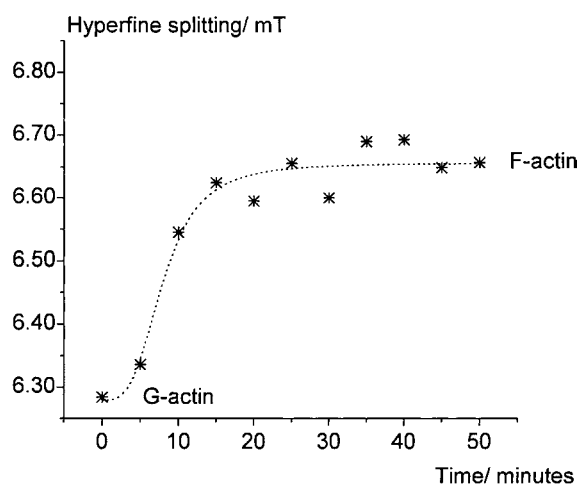


Fig. 3. Temporal course of the polymerization of actin. The hyperfine splitting ($2A'_{zz}$) is plotted as a function of time. Zero time corresponds to the addition of 100 mM KCl and 2 mM $MgCl_2$ to induce polymerization.

collective motions are already in the time range of the biological functions, and the transition between two functionally distinct states must have a low-energy pathway [17]. In actin, the two larger domains exhibit a scissor-type opening of the nucleotide-binding cleft; this motion and, thereby, the entire protein structure is stabilized by ATP in G-actin and by ADP in F-actin [18].

The unfolding of G- and F-actins is a complex process characterizing more than one discrete molecular regions with different thermal stabilities (Figs. 4 and 5; [7]). In order to have the precise description of their unfolding, deconvolution of the DSC thermograms was performed using suitable computer software. Table 1 summarizes the temperature transitions

Table 1
Parameters of the thermal transitions in skeletal muscle actin

Form of actin	Transition temperature/ $^{\circ}C$ ^a	Transition enthalpy/(mJ/g)	
		measured	deconvoluted
G-actin	47.3	304 (total)	184
	53.4		120
F-actin	59.7	550 (total)	171
	60.6		231
	61.3		148

^a Transition temperatures were obtained from the deconvoluted data.

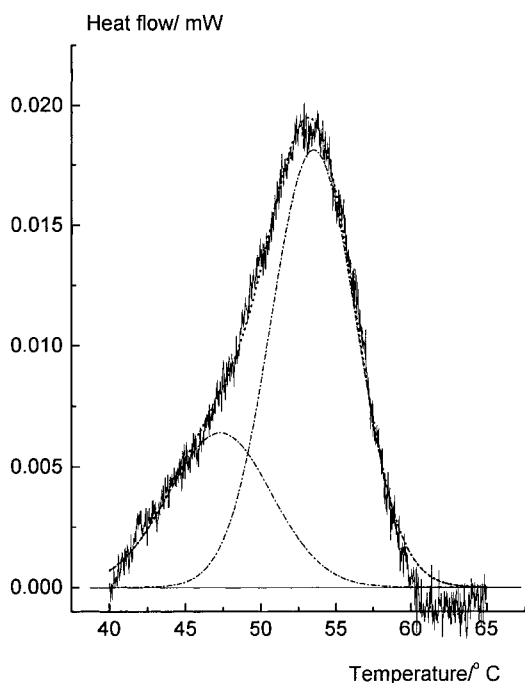


Fig. 4. DSC scan of G-actin. Note the broad unfolding of monomeric actin. Symbols: (—), composite transitions; and (···), resulting thermal transition.

and enthalpies of G- and F-actins. Considering the structure and the protein dynamics simulation, it is reasonable to assume that the lower transition (47.3°C) arises from subdomains 2 and 4, whereas the higher transition at 53.4°C can be assigned to subdomains 1 and 3. The latter structural units have similar basic fold: a central five-stranded β -sheet is surrounded by three α -helices, probably the result of gene duplication and fusion [2].

Studying F-actin, the deconvolution resulted in three transitions: at $T_m=59.7^\circ$, 60.6° and 61.3°C , with a larger total enthalpy. The melting curve is much sharper than that of the G-actin, and it is shifted to higher temperature. The range of the thermal transition is ca. 20°C in the case of G-actin, the much sharper range (6°C) of F-actin is due to the strong intermonomer interaction. It can be supposed that the highest transition at 61.3°C represents the intermonomer interaction. The general increase of the unfolding temperatures is the consequence of the larger structural stability of the filamentous form in comparison to

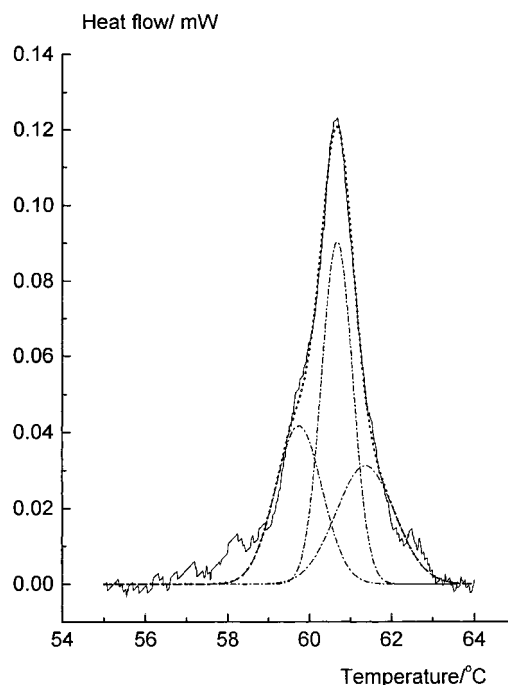


Fig. 5. Thermal transition of polymerized actin. In comparison to G-actin, the unfolding of the protein is much sharper and the transition is shifted to higher temperatures. Symbols: (—) composite transitions; and (···) resulting thermal transition.

globular form. It is interesting to note that the calorimetric enthalpy of the main transition agrees well with the van't Hoff enthalpy calculated from the EPR data. This suggests that the main transition represents the thermal denaturation of subdomains 1 and 3, and supports the assumption about the thermal transition of at least two independent domains, based on our calorimetric data, which is in good agreement with structural X-ray diffraction results [13].

3.3. Internal dynamics of actin filaments

Actin is a cytoplasmic protein which has a large functional diversity. According to data in the literature, actin is highly dynamic in cells and its properties are modulated by environmental signals [19].

Earlier studies using electron microscopic and spectroscopic techniques suggest a strong correlation between structural disorder and flexibility of actin [20–22]. Locally, F-actin filaments may significantly deviate from a perfect helical structure, and it can be

assumed that the number of these structural disorders increases with increasing temperature. Therefore these structural deviations may contribute to the increased torsional flexibility of the filaments derived from EPR measurements.

Analysis of the thermal stability for the two actin forms (G- and F-actins) indicated relatively simple heat capacity profiles that reflect the stabilizing forces acting in the protein structure between amino acid side chains, protein segments or domains. It is known that actin monomer consists of structural domains which are separated by a cleft, and the bound nucleotide is localized in the cleft [2,8,13]. Investigation of the internal dynamics showed that the large and small domains of G-actin move as two units relative to one another [18]. It can be assumed that the two components obtained by the deconvolution procedure for G-actin correspond to the thermal unfolding of the subdomains comprising these structural units. The higher thermal transition can be assigned to subdomains 1 and 3. This is supported by the spectroscopic measurements. The maleimide labels that report the local structural changes are rigidly attached to Cys-374 in subdomain-1 and showed a rapid change of the rotational mobility at 54°C which is the sign of the unfolding. Polymerization of actin was accompanied by a significant increase of T_m and ΔH , implying that the monomer–monomer interaction enhances the thermal stability [6,7]. The EPR results reflected similar changes of the thermodynamic parameters, namely that the structural stability increased upon polymerization due to strong monomer–monomer interaction.

Our finding that the DSC scans of F-actin can be decomposed into three parts seems to be in good agreement with the structure of F-actin proposed by Holmes et al. [14]. According to their plausible model for F-actin, the large domain fits rather naturally along the long two-start actin helix and the interactions are intensive between the molecules along it. The strong interaction is brought about by the formation of an extensive hydrophobic core between neighbouring molecules along the two-start helix into which the molecules from the opposite strand are involved in a three-bodied way. The myosin-binding residues form

a patch near the filament. In this way, the lower component of DSC scan could be attributed to the small domain, the middle one to the large one and the higher temperature component could originate from the strong hydrophobic core to stabilize the filament.

Acknowledgements

This work was supported by research grants from ETT T-06 017/96, OTKA CO 123, CO 272 and INCO COPERNICUS EU ERBIC 15CT960821.

References

- [1] E.D. Korn, *Physiol. Rev.* 62 (1982) 672.
- [2] W. Kabsch, K.C. Holmes, *FASEB J.* 9 (1995) 167.
- [3] J.A. Barden, C.G. dos Remedios, *Eur. J. Biochem.* 146 (1985) 5.
- [4] M. Mossakowska, J. Belagyi, H. Strzelecka-Golaszewska, *Eur. J. Biochem.* 175 (1988) 557.
- [5] F. Oosawa, in A. Stracher (Ed.), *Muscle and Nonmuscle Motility*, Vol. 1, Academic Press, New York, 1983, pp. 115.
- [6] A. Bertazzon, G.H. Tian, A. Lamblin, T.Y. Tsong, *Biochemistry* 29 (1990) 291.
- [7] D. Lőrinczy, J. Belagyi, *Thermochim. Acta* 259 (1995) 153.
- [8] J.A. Spudich, S. Watt, *J. Biol. Chem.* 246 (1971) 4866.
- [9] P. Fajer, D. Marsh, *J. Mag. Res.* 49 (1982) 212.
- [10] D.D. Thomas, L.R. Dalton, J.S. Hyde, *J. Chem. Phys.* 65 (1976) 3006.
- [11] L.I. Horváth, D. Marsh, *J. Mag. Res.* 80 (1988) 314.
- [12] T.C. Squier, D.D. Thomas, *Biophys. J.* 49 (1986) 921.
- [13] W. Kabsch, H.G. Mannherz, D. Schuck, E.F. Pai, K.C. Holmes, *Nature* 347 (1990) 37.
- [14] K.C. Holmes, D. Popp, W. Gebhard, W. Kabsch, *Nature* 347 (1990) 44.
- [15] S. Fujime, S. Ishiwata, *J. Mol. Biol.* 62 (1971) 251.
- [16] J.A. McCammon, *Rep. Prog. Phys.* 47 (1984) 1.
- [17] B.F. Rasmussen, A.M. Stock, D. Ringe, G.A. Petsko, *Nature* 357 (1992) 423.
- [18] M.M. Tirion, D. ben-Avraham, *J. Mol. Biol.* 230 (1993) 186.
- [19] P. Shterline, J.C. Sparrow, *Protein Profile Vol. 1*. Academic Press, London (1994), pp. 1–121.
- [20] D.L. Stokes, D.J. DeRosier, *J. Cell Biol.* 104 (1987) 1005.
- [21] A. Bremer, R.C. Millonig, R. Sütterlin, A. Engel, T.P. Pollard, *J. Cell Biol.* 115 (1991) 689.
- [22] H.P. Erickson, *J. Mol. Biol.* 206 (1989) 465.